IEEE Access
Multidisciplinary | Rapid Review | Open Access Journal

Received October 20, 2018, accepted November 10, 2018, date of publication November 21, 2018,
date of current version December 27, 2018.

Digital Object Identifier 10.1109/ACCESS.2018.2882644

Experimental Characterization of Millimeter-Wave Indoor Propagation Channels at 28 GHz

GUOJIN ZHANG[1], KENTARO SAITO[2], WEI FAN[1], XUESONG CAI[1], PANAWIT HANPINITSAK[2], (Student Member, IEEE), JUN-ICHI TAKADA[2], (Senior Member, IEEE), AND GERT FRØLUND PEDERSEN[1]

[1]Antennas, Propagation and Millimetre-Wave Systems Section, Department of Electronic Systems, Faculty of Engineering and Science, Aalborg University, 9220 Aalborg, Denmark
[2]Department of Transdisciplinary Science and Engineering, School of Environment and Society, Tokyo Institute of Technology, Tokyo 1528550, Japan

Corresponding author: Wei Fan (wfa@es.aau.dk)

This work was supported by Huawei Technologies and the VIRTUSUO Project funded by the Innovation Fund Denmark. The work of W. Fan was supported by the Danish Council for Independent Research under Grant number: DFF611100525.

ABSTRACT The increasing requirement for the mobile data traffic accelerates the research of millimeter-wave (mm-wave) for future wireless systems. Accurate characterization of the mm-wave propagation channel is fundamental and essential for the system design and performance evaluation. In this paper, we conducted measurement campaigns in various indoor scenarios, including classroom, office, and hall scenarios, at the frequency bands of 27–29 GHz. The spatial channel characteristics were recorded by using a large-scale uniform circular array. A high-resolution parameter estimation algorithm was applied to estimate the mm-wave spherical propagation parameters, i.e., the azimuth angle, elevation angle, delay, source distance, and complex amplitude of multipath components. With the same measurement system, the channel parameters including decay factor, delay spread, angular spread, and line of sight power ratio are investigated thoroughly in individual indoor scenarios and compared in different indoor scenarios. Furthermore, the impact of the furniture richness level and indoor geometry on the propagation parameters are also investigated.

INDEX TERMS Decay factor, delay spread, angular spread, LOS power ratio, millimeter-wave, channel sounding.

I. INTRODUCTION

The utilization of millimeter-wave (mm-wave) frequencies for the fifth generation communications (5G) and beyond has gained considerable interest in both academic and industrial community recently due to the spectrum scarcity at the sub-6 GHz frequency bands [1]–[4]. Mm-wave frequency bands have been identified as the promising candidate frequencies for future cellular networks [2]. However, the mm-wave propagation characteristics are very different from that observed in the sub-6 GHz frequency bands. Accurate understanding of the mm-wave propagation channels are essential and have attracted increasing attention recently [5]–[7].

Extensive measurement campaigns have been conducted at mm-wave frequency bands [8]–[15]. In [8] and [9], measurement campaigns were conducted in high-speed trains scenarios, and extensive ray tracing simulations were applied to understanding the propagation mechanisms. In [10], the measurement was performed at 81−86 GHz (E-band) in a street canyon scenario, and a geometry-based single-bounce channel model was developed for investigating the characteristics in the delay domain. Considerable efforts have been devoted to study the channel characteristics at 60 GHz frequency bands [11]–[13], which have been exploited for unlicensed wireless HD and Wireless Gigabit Alliance (WiGig) WLAN applications [14] with Gbps transmission in short range indoor communications. In addition, several radio channel sounding campaigns were performed at 60 GHz and 70 GHz frequency bands in various short-range scenarios, including offices, shopping mall and station in [15]. Furthermore, various investigations for the propagation channels at the frequency bands of 28 GHz have been conducted [16]–[18]. Channel characteristics such as path loss,

TABLE 1. Measurement setup.

Room	R1-Classroom [20]	R2-Classroom	R3-Office	R4-Hall
Dimension (m^3)	$8.54 \times 6.70 \times 2.71$	$8.54 \times 6.70 \times 2.71$	$4.78 \times 3.44 \times 2.85$	$39 \times 20 \times 10$
Tx antenna	Biconical antenna A	Biconical antenna A	Biconical antenna B	Biconical antenna A
Rx antenna	Biconical antenna B	Biconical antenna B	Biconical antenna A	Biconical antenna B
Center frequency	28 GHz	28 GHz	28 GHz	28 GHz
Transmit power	15 dBm	12 dBm	15 dBm	15 dBm
Tx\Rx antenna height	1.50 m	1.30 m	1.50 m	1.50 m
Frequency sweep points	360	360	360	360
UCA radius	0.24 m	0.24 m	0.24 m	0.24 m
Details	20 positions	Remove and restore tables and chairs	Remove contents and shelves	20 positions

signal outage [16], reflection coefficients, penetration losses caused by common building materials [17] and angular characteristics [18] have been thoroughly analyzed. More recently, in [19], measurements in two important cellular scenarios, i.e., an urban microcell and an open indoor hall, were conducted at the frequency bands of 28 GHz, with a focus on spatio-temporal channel characteristics parameters.

Although extensive measurement efforts have been taken to understand the propagation channels, most of them were performed in a single scenario, e.g. the indoor scenario or the outdoor scenario. Furthermore, the frequency bands and measurement configurations differ in these works. This poses challenge on understanding the influence of different scenarios on the mm-wave propagation characteristics. To the authors' best knowledge, the comparison among the mm-wave propagation characteristics observed in several different scenarios with the same measurement system and frequency band applied has not been investigated so far. Moreover, it is usually expensive and difficult to carry out channel measurement at mm-wave frequency bands. Thus, simulation tools such as ray tracing have been widely exploited to predict the channel behaviors. However, the simulation accuracy relies on the realistic modeling of the various objects existing in the environment, i.e. the detailed database of electrical properties for the structure and random minor objects. This also necessitate the measurement-based investigation for the impact of the furniture richness level and indoor geometry on the radio propagation parameters.

In this paper, the mm-wave propagation channels in different indoor scenarios including classroom, office and hall are recorded by using the same measurement system. The measurement system is based on the virtual antenna array scheme to sound the mm-wave channel at the frequency band of 27 GHz-29 GHz. Channel characteristics, including power delay profiles (PDPs), decay factor, delay spread, angular spread and line of sight (LOS) power ratio are thoroughly investigated in individual scenarios and compared among different scenarios. Moreover, we also gain insights into the impact of the indoor geometry, materials and furniture richness level on the channel characteristics.

The rest of the paper is organized as follows. Section II describes four measurement campaigns. Section III briefly describes the post-processing for extracting the parameters of interest. The resulted channel models are discussed in Section IV. Finally, Section V concludes the paper.

II. MEASUREMENT CAMPAIGN

In this section, the measurement scenarios and setup of the four indoor measurements are detailed. The scenarios include two classroom scenarios, an office scenario and a hall scenario, with measurement settings specified in Table 1.

A. MEASUREMENT SETUP

The measurement system is a vector network analyzer (VNA) based virtual array channel sounding system. Readers can refer to [20] and [21] for details. Two types of biconical antenna are used in the measurements, which are commercial biconical antenna SZ-2003000/P (marked as A) [22] and homemade biconical antenna (marked as B) [23]. Both biconical antennas are wideband and omnidirectional in the horizontal plane and has narrow elevation patterns in elevation plane. The antenna gains of commercial and homemade biconical antennas are 6 dB and 4.8 dB at 28 GHz, respectively. The biconical antenna is rotated clockwise on a rotating pedestal with a pre-set radius (as shown in Table 1) with 1 degree rotating steps to form a UCA for the four measurement campaigns. In the measurements, the channel propagation from 27-29 GHz was swept by using the VNA, giving a delay resolution of 0.5 ns. 750 frequency points were collected, limiting the maximum delay to 375 ns.

B. MEASUREMENT SCENARIO

1) R1-CLASSROOM

The measurement was performed in a typical small classroom [20] as shown in Fig. 1, where three sides of the room are covered by the concrete walls and three windows on the other side. The height of the tables is 0.74 m. A total

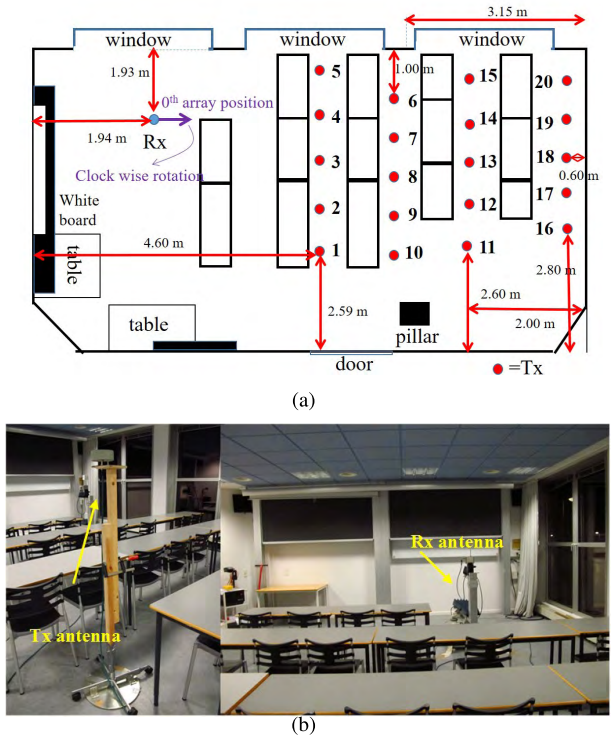

(a)

(b)

FIGURE 1. (a) The sketch of R1-Classroom with 20 Tx locations. (b) The photograph of R1-Classroom and Tx (left), Rx (right) antennas.

of 20 spatial snapshots (i.e. locations) were measured by moving the Tx antenna between the tables. Each Tx location in each row was spaced 0.8 m apart. An illustration of the classroom and antennas used in R1-Classroom are presented in Fig. 1.

2) R2-CLASSROOM

The measurements were performed in the same classroom as R1-Classroom, where the Tx antenna was fixed at the corner and Rx antenna set in the center of the classroom, as shown in Fig. 2. In the measurement, we removed four tables and chairs in the classroom and repeated the measurements for each step (in 5 steps). Then we restored and brought back two or four tables and chairs and repeated the measurements for each step (in 5 steps). The classroom is full of tables and chairs in step 1 and 10, and totally empty in step 4 and 7. The last measurement was conducted with the classroom totally empty and all blind windows open as shown in Fig. 2(c). The objective is to investigate the impact of tables and chairs on the channel characteristics.

3) R3-OFFICE

To study the impact of furniture richness level on the channel characteristics, we performed measurements in a typical office scenario, which is equipped with metallic shelves and loaded with books, as shown in Fig. 3. In the measurement, we removed the contents on the shelves one by one from step 2 to step 6 and then removed shelves from step 7 to step 11.

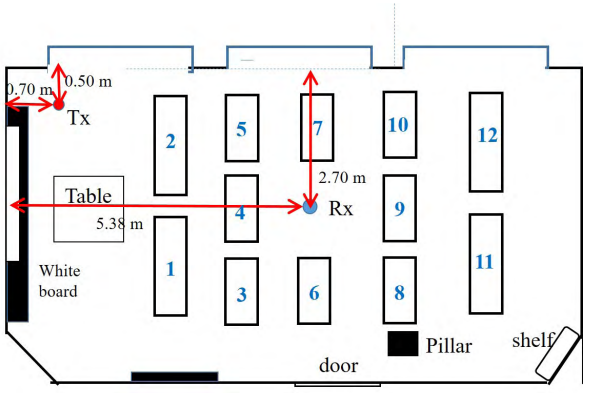

(a)

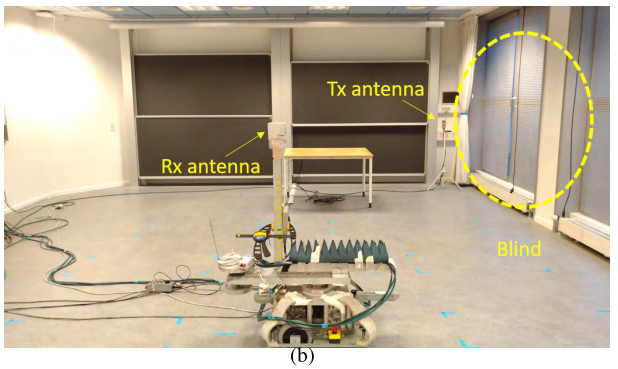

(b)

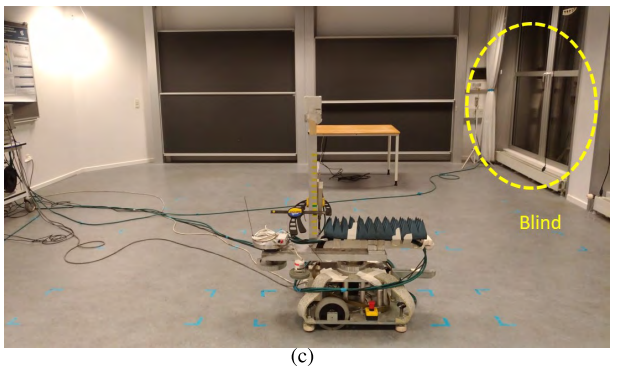

(c)

FIGURE 2. (a) The sketch of R2-Classroom with 12 tables. (b) The photograph of R2-Classroom and Tx/Rx antennas location with all room furniture removed. (c) The photograph of empty R2-Classroom with blind windows open.

A total of 11 measurements were performed in the campaign, starting from fully loaded shelves in step 1 and ending with no shelves in the room in step 11.

4) R4-HALL

To investigate the channel characteristics in irregular large indoor scenarios, the measurement was conducted in a hall scenario, as shown in Fig. 4. The shape of the hall is irregular, and the ceiling of the hall is 10 m high. There is also a big table and stairs along the south wall. The four big ventilation tubes (shown as yellow circles) and six pillars (shown as white circles) are located around the hall. The Rx was located near the four big pillars in the west side of the hall, and the Tx

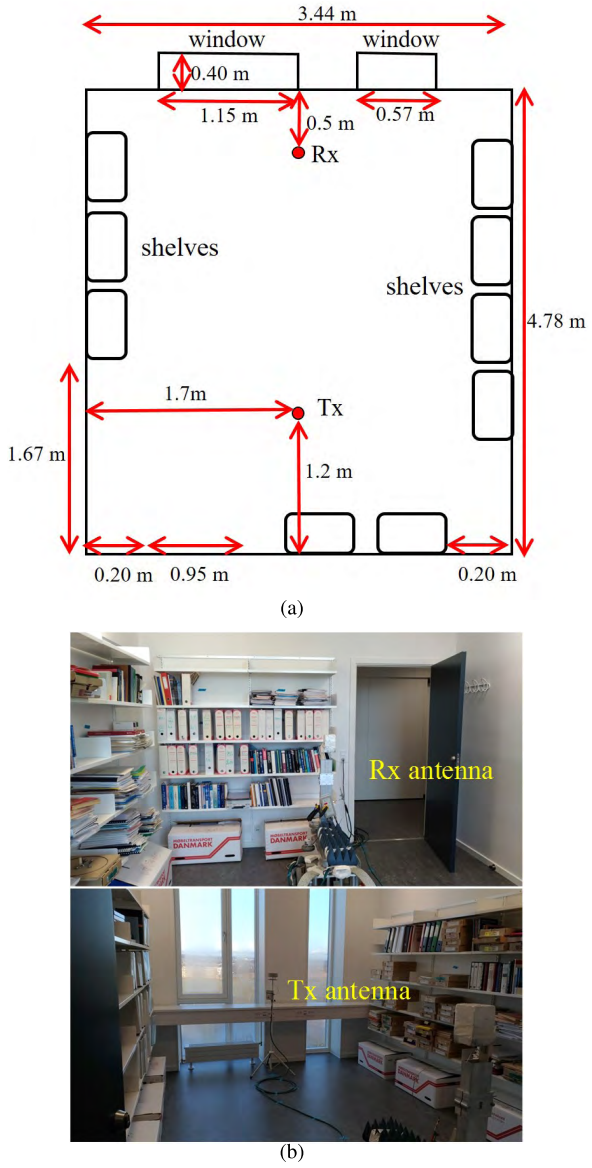

FIGURE 3. (a) The sketch of R3-Office. (b) The photograph of R3-Office and Tx (down), Rx (top) antennas.

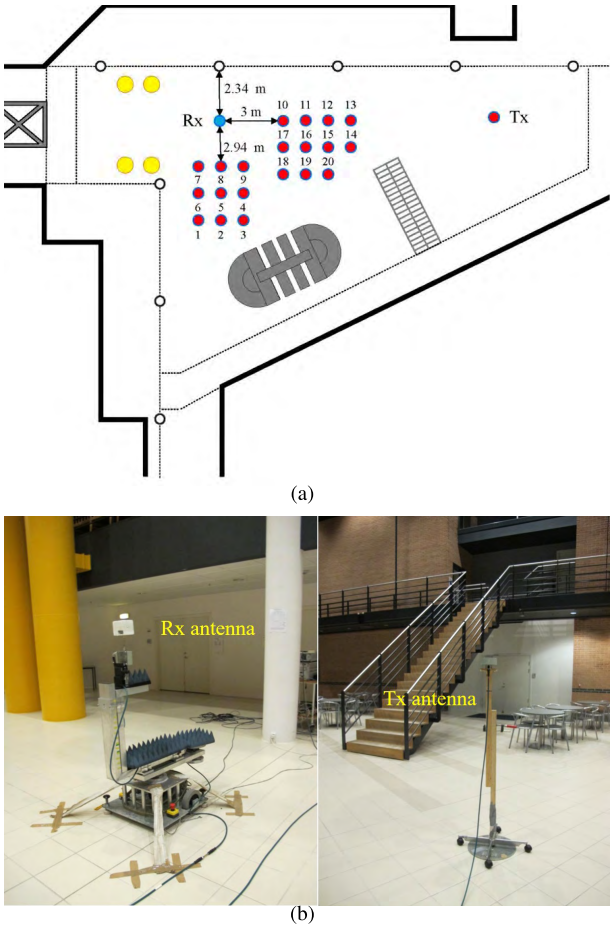

FIGURE 4. (a) The sketch of R4-Hall with 20 Tx locations. (b) The photograph of R4-Hall and Rx (left), Tx (right) antennas.

was located at 20 different points distributed around the Rx, as shown in Fig. 4. Each Tx location is 1 m apart from each other.

III. PARAMETER ANALYSIS

A. POWER DECAY FACTOR

When modeling the radio propagation channel, the PDPs are expressed as a combination of primary and decay components [15], [24]. The primary component contains the direct propagation and possibly first-order reflections, and the decay component is from the specular spectrum and distributed diffuse scattering. The decay tail of the power-delay profile can be typically modeled as a tail with an exponential decay rate, defined as decay factor β.

As explained, the Rx antenna was mounted at uniform angles around a circle to obtain a UCA with $N = 360$ elements, and $M = 750$ frequency points were recorded for each frequency band. The Hanning window and the inverse Fourier transom (IFT) computation are used to processing the raw data in the frequency domain. The average power delay profiles (APDPs) can be obtained by

$$P_m(\tau) = \frac{1}{N}\sum_{n=1}^{N} \left|h_{m,n}(\tau)\right|^2 \tag{1}$$

where $h_{m,n}(\tau)$ represents the channel impulse response (CIR) at m-th sample in delay domain, and n-th measured element.

For the accuracy of analysis, we need to define the fixed range of the linear regression of the decay tail. The end time of the regression line τ_{noise} corresponds to the noise floor P_{noise}. The beginning of the linear regression fit line $\bar{\tau}$ can be defined as [25]

$$\bar{\tau} = \frac{\sum_{m=1}^{M} P_m(\tau)\cdot\tau}{\sum_{m=1}^{M} P_m(\tau)}, \tag{2}$$

where P_m is the power value of the APDPs at m-th delay sample.

According to the regression line, we obtain the slope of the decay tail and decay factor β, which can be described as [25]

$$\beta = -\frac{10\log(e)}{s}, \tag{3}$$

where e is Eulers number, and s is the slope of the power decay tail in APDPs, represented as dB/ns.

B. DELAY SPREAD

The delay spread of the channels is widely used for characterizing the multipath components (MPCs) richness in the wireless channel, which is calculated as the second-order central moments of the APDPs [26]. The mean delay $\bar{\tau}$ is defined in (2), and root mean square (RMS) delay spread σ_τ can be computed from the measured as [26]

$$\sigma_\tau = \sqrt{\frac{\sum_{m=1}^{M} P_m(\tau)\cdot\tau^2}{\sum_{m=1}^{M} P_m(\tau)} - \bar{\tau}^2}. \tag{4}$$

C. ANGLE SPREAD

In this paper, we utilized the HRPE algorithm [27] to estimate the mm-wave spherical propagation parameters of the UCA channels, i.e. azimuth angle, elevation angle, delay, source distance and amplitude of MPCs. Then the spatial-temporal CIR $h(\tau,\theta,\phi,d)$ can expressed as

$$h(\tau,\theta,\phi,d) = \sum_{l=1}^{L} \alpha_l \delta(\tau-\tau_l)\delta(\theta-\vartheta_l)\delta(\phi-\varphi_l)\delta(d-d_l), \tag{5}$$

where L is the number of spherical waves impinge into the UCA, τ_l is the propagation delay, ϑ_l and φ_l represent the azimuth and elevation angles of the l-th path, respectively. α_l denotes the complex amplitude, and d_l is the propagation distance between the UCA center and the last source point during the propagation route of the l-th path, respectively.

As most of the estimated elevation angles are close to 90 degree, we only focus on the azimuth angles. Then the spatial-temporal CIR can be expressed as $h(\tau,\varphi)$. The circular angle spread σ_φ can be calculated, as defined in [27] and [28],

$$\sigma_\varphi = \sqrt{-2\log\left(\left|\frac{\sum_{l=1}^{L}\exp(j\varphi_l)\cdot|h(\tau_l,\varphi_l)|^2}{\sum_{l=1}^{L}|h(\tau_l,\varphi_l)|^2}\right|\right)}. \tag{6}$$

D. LOS POWER RATIO

To figure out the dominant components of the channel, the LOS power ratio K is defined as the ratio of the power in the LOS component or most dominant component to the power in the non-line of sight (NLOS) or the other MPCs components [26]. LOS power ratio plays a vital role in estimating statistics, which is identified as,

$$K = \frac{P_{\mathrm{LOS}}(\tau)}{P_{\mathrm{NLOS}}(\tau)} \tag{7}$$

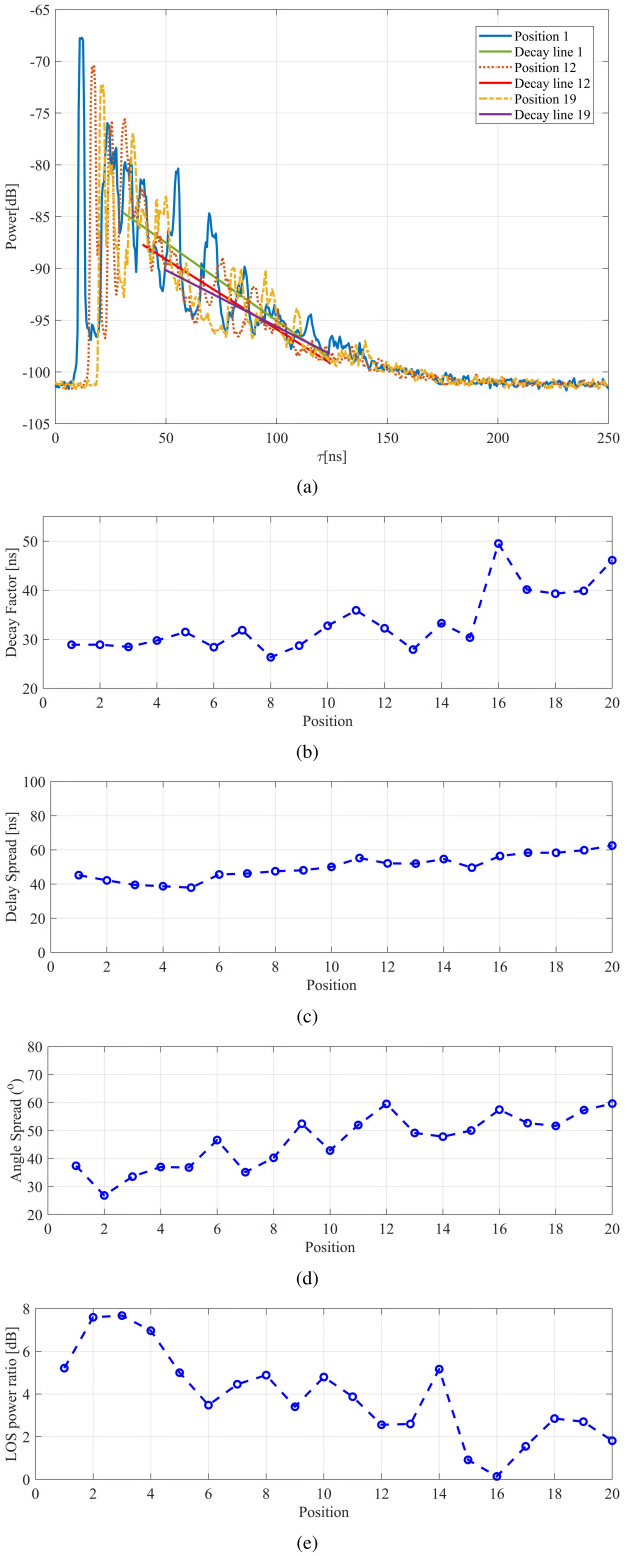

FIGURE 5. The channel characteristics of total 20 Tx locations observed at 27 GHz-29 GHz in R1-Classroom. (a) APDPs. (b) Decay factor. (c) Delay Spread. (d) Angle Spread. (e) LOS power ratio.

where, $P_{\mathrm{LOS}}(\tau)$ is the power of LOS path (i.e. in most dominant component) and $P_{\mathrm{NLOS}}(\tau)$ is the sum of the power of all the MPCs components except the most dominant path.

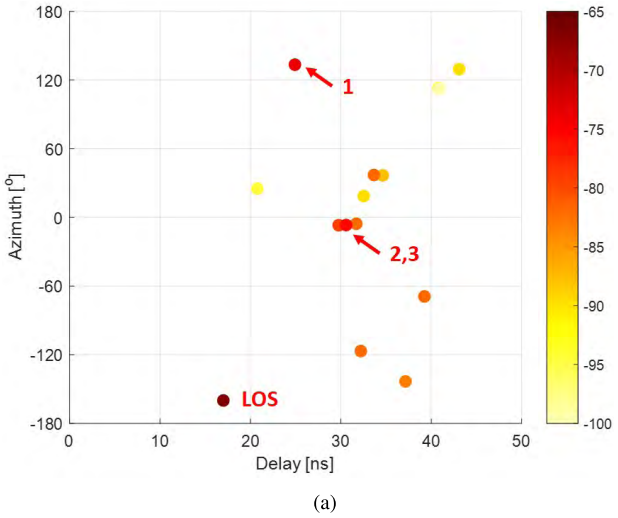

(a)

FIGURE 6. The PADPs of Tx position 12 at 27 GHz-29 GHz in R1-Classroom.

IV. MEASUREMENT RESULTS

A. R1-CLASSROOM

The calculated APDPs with corresponding decaying lines at Tx positions 1, 12, and 19 at 27 GHz-29 GHz in R1-Classroom are illustrated in Fig. 5(a) for an example. It can be observed from Fig. 5(a) that, the strongest path is contributed by LOS propagation, with power values of −67.7 dB, −69.4 dB and −72.3 dB with Tx at position 1, 12 and 19, respectively. The power of the LOS path decreases, as the distance between the Tx and Rx increases for the three example locations. The noise level is about −100 dB, leading to the dynamic range around 30 dB.

The characteristic parameters of total 20 Tx locations are plotted in Fig.5(b)-5(e). It can be observed that the values of decay factor β in Fig. 5(b), delay spread in Fig. 5(c) and angle spread in Fig. 5(d) are relatively lower at position 1-5 than other positions and the values of LOS power ratio in Fig. 5(e) are higher than others. That is due to the fact that dominant LOS path has less path loss and strong reflections from the whiteboard and windows at position 1-5.

It is also found that the values of decay factor β, delay spread and angle spread are higher and the values of LOS power ratio are lower at positions 16-20 than other positions. That is probably due to the fact that the distance between Tx and Rx antenna is much larger, and the Tx antenna is much closer to the back wall with the distance of 0.6 m at the positions 16-20, leading to the lower power of the LOS path and richer multipath components from the back walls.

The power angle delay profiles (PADPs) of position 12, corresponding to the position with the highest angle spread, is shown in Fig. 6. The large difference in angle spread among locations is most likely caused by the difference in path 1 (reflection from the windows) and path 2,3 (from the whiteboard on the west wall) among locations.

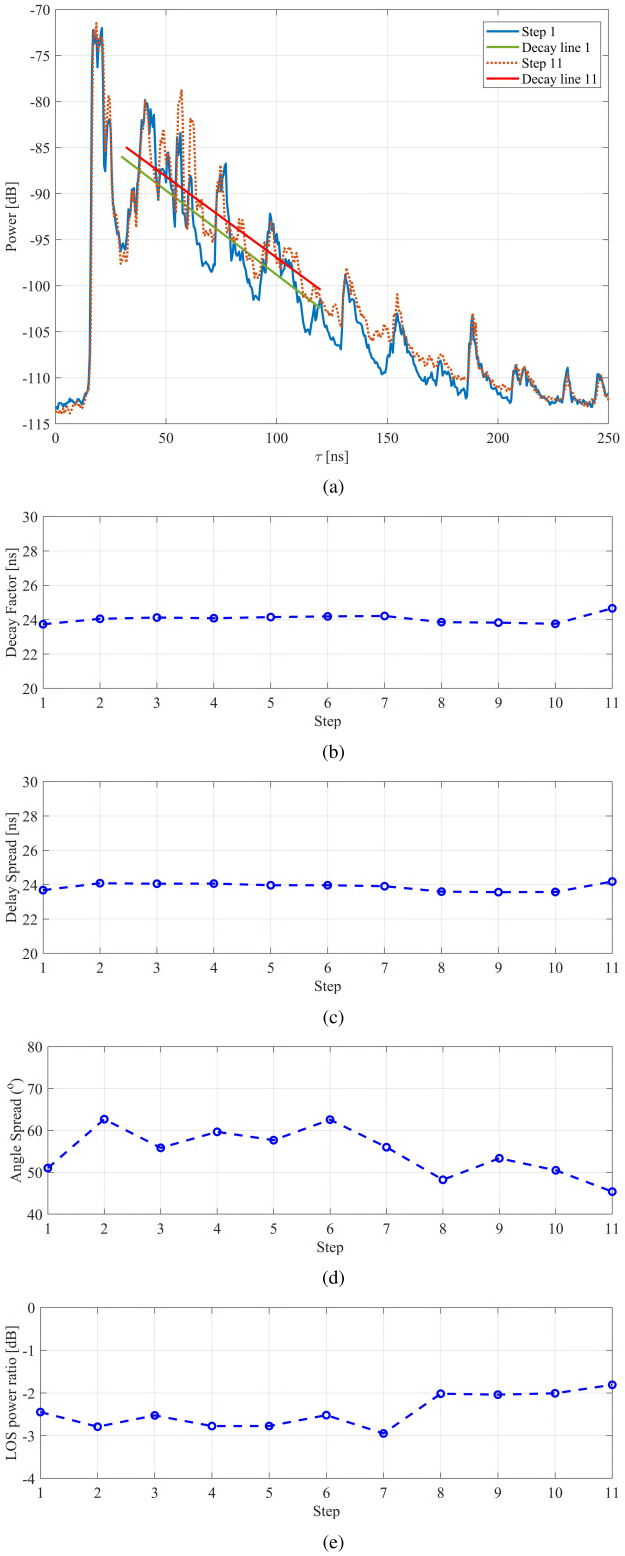

(a) (b) (c) (d) (e)

FIGURE 7. The channel characteristics of 11 steps at 27 GHz-29 GHz in R2-Classroom. (a) APDPs. (b) Decay factor. (c) Delay Spread. (d) Angle Spread. (e) LOS power ratio.

B. R2-CLASSROOM

The APDPs with corresponding decaying lines of the measurement step 1 and 11 measured in R2-Classroom at

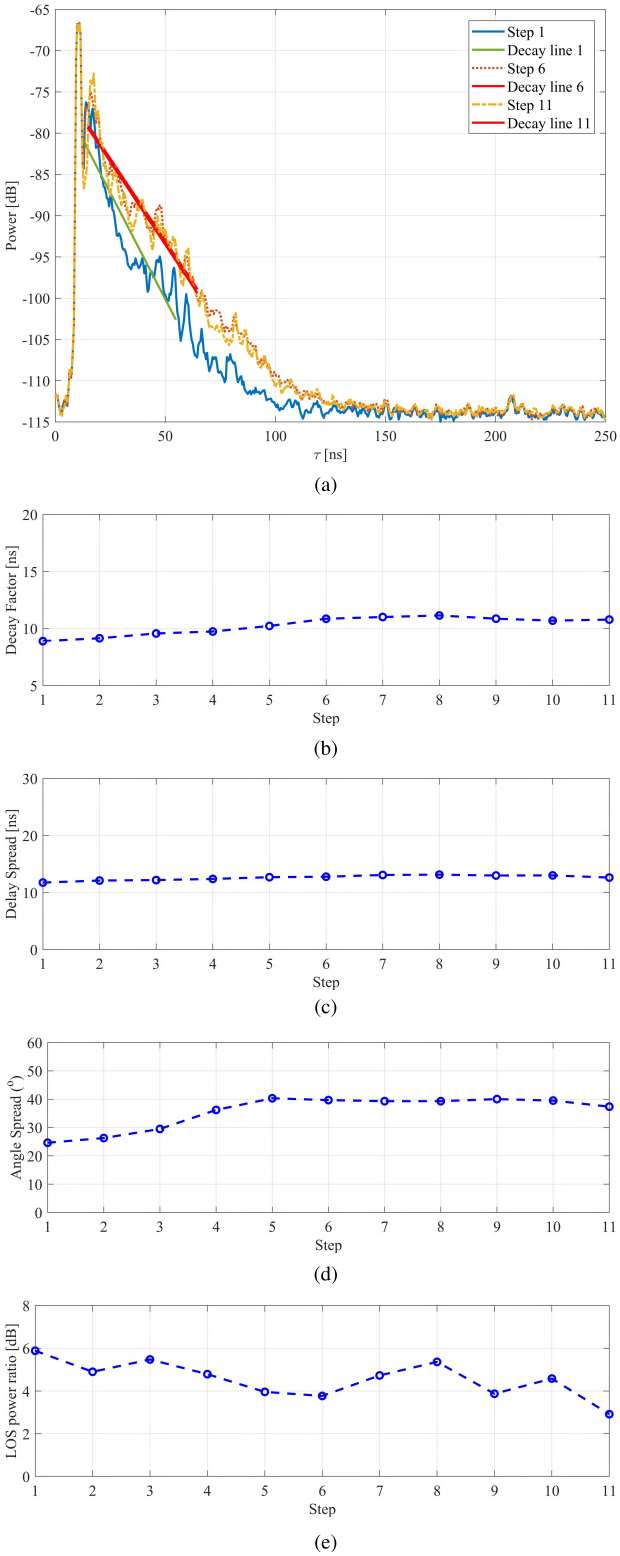

FIGURE 8. The channel characteristics of 11 steps at 27 GHz-29 GHz in R3-Office. (a) APDPs. (b) Decay factor. (c) Delay Spread. (d) Angle Spread. (e) LOS power ratio.

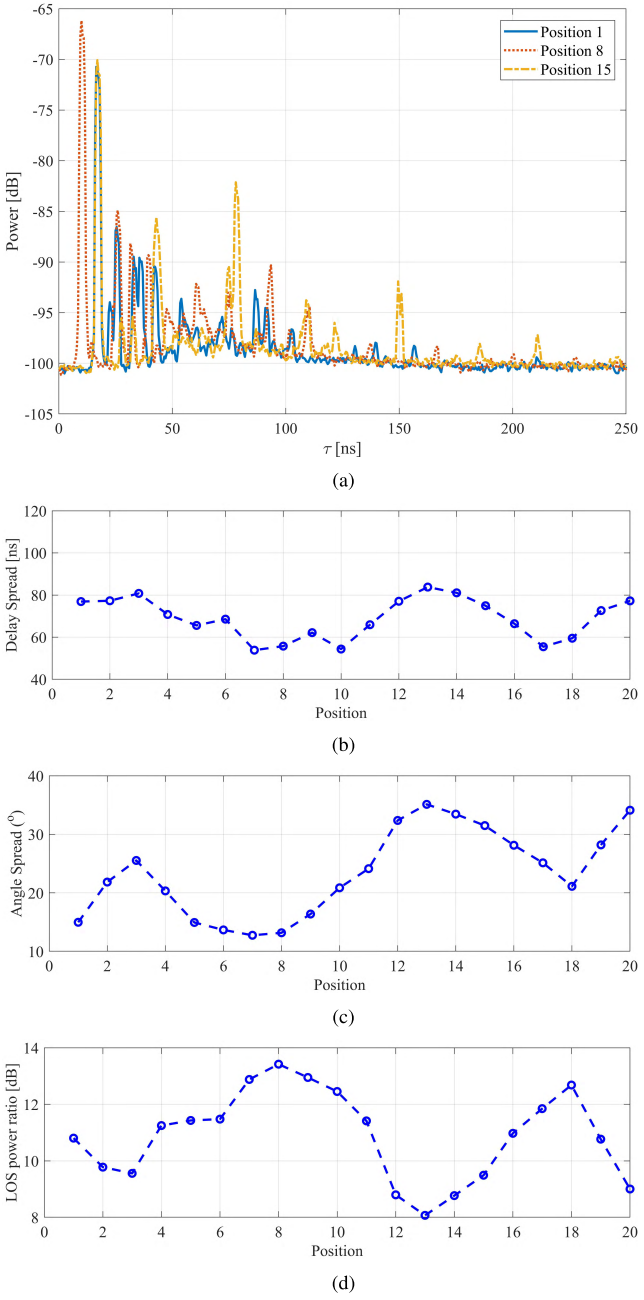

FIGURE 9. The channel characteristics of 20 positions at 27 GHz-29 GHz in R4-Hall. (a) APDPs. (b) Decay factor. (c) Delay Spread. (d) Angle Spread. (e) LOS power ratio.

27 GHz-29 GHz are described in Fig. 7(a) for an example, which show little relationship with the furniture moving out and in on the decay lines. Two strongest paths with the same power values of about −66.7 dB are found in APDPs shown in Fig.7(a). The two strongest paths are from LOS propagation and probably strong reflection from the corner, respectively. The strong reflection may be from the poles of the blackboard, as they are aluminum which reflects the radio wave well.

The characteristic parameters of total 11 steps are shown in Fig. 7(b)-7(e). With removing the tables and chairs and moving back in the classroom, the values of decay factor β in Fig. 7(b) and delay spread in Fig. 7(c) remains stable. It can be observed that, there is little influence on the propagation channel for our measurements. One possible reason is that

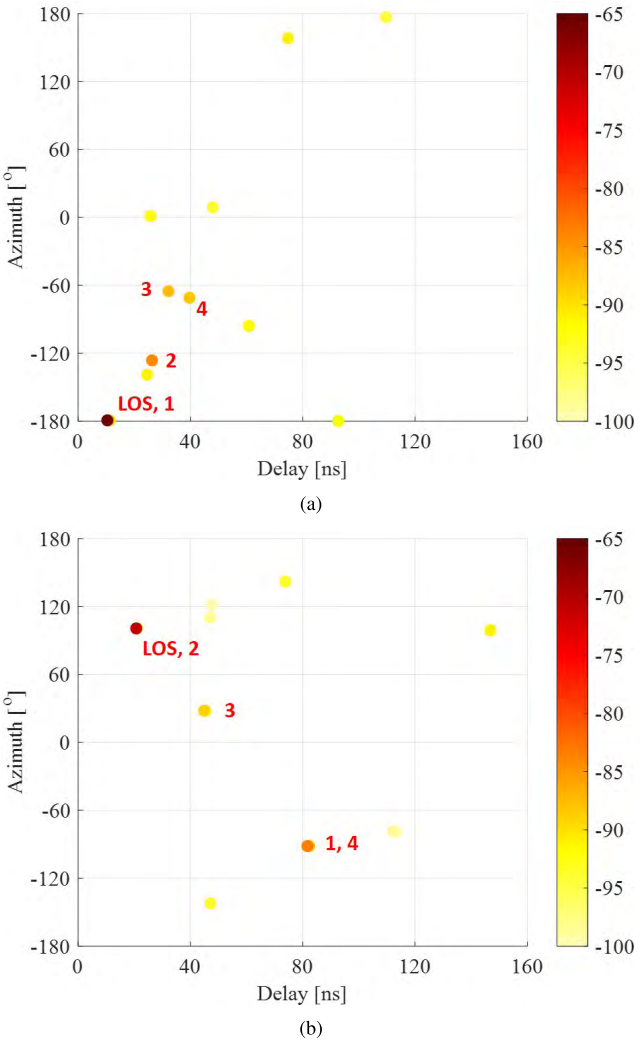

FIGURE 10. The PADPs of Tx positions 8 and 14 at 27 GHz-29 GHz in R4-Hall. (a) Position 8 (b) Position 14.

the Tx and Rx antennas were located higher than the objects in the room, resulting in little interaction between the objects and multipath components. The elevation half power beam width of commercial biconical is narrow, leading to the low power of reflection and scattering from tables.

It is noticed that with blind windows open in step 11, there will be small difference in the values of the decay factor in Fig. 7(b), delay spread in Fig. 7(c) and angle spread in Fig. 7(d), which is perhaps due to the strong reflections from the open blind windows in the corner.

The similar tendency has been observed in Fig. 7(e) that the values of LOS power ratio are distributed in the range between −2 and −3 dB, indicating that the measurements in the classroom are all not LOS dominated. That is because of the strong reflection from the aluminous poles of the blackboard near the Tx located, with almost the same power of the LOS path propagation.

C. R3-OFFICE

Fig. 8(a) shows the APDPs with corresponding decaying lines of step 1, 6 and 11, which again shows slight relationship with the furniture richness in the office. The strongest paths of each step are from LOS path propagation, with the same power values of −66.7 dB. As we remove the contents on the shelves till with only shelves in step 6, the power level of specular paths is higher than fully occupied in step 1 shown in Fig. 8(a). When we continue to remove the shelves till empty office in step 11, the power level of specular paths remains stable, due to the fact that the surface of the shelves is relatively small compared with the surface of the walls.

The characteristic parameters of total 11 steps measured in R3-Office at 27 GHz-29 GHz are plotted in Fig. 8(b)-8(e). The similar tendency has been observed in Fig. 8(b)-8(e), with minor variations in the values of decay factor, delay spread, angle spread and LOS power ratio, respectively. For the measurement steps from 1 to 6, the values of decay factor, delay spread and angle spread increase slightly and the values of LOS power ratio decrease, mostly due to the fact that less waves will be absorbed by the contents on the shelves, as the contents are removed from the shelves one by one. An explanation for the values of decay factor, delay spread, angle spread remain stable from step 7 to 11, is that the surfaces of the shelves are relatively small comparing with the walls, leading to little impact on the MPCs components in the office.

D. R4-HALL

The APDPs with corresponding decaying lines at position 1, 8, 15 measured in R4-Hall scenario at 27 GHz-29 GHz are plotted in Fig. 9(a) for an example. It can be observed that there is little diffuse spectrum in Fig. 9(a), due to the large dimension of the hall scenario. In this case, it makes no sense to study the decay factor in such large hall scenario, since the multipath components are dominated by specular components, with little diffuse components.

The characteristic parameters of total 20 Tx positions are shown in Fig. 9(b)-9(d). It is observed that the values of delay spread and angle spread are relatively low as shown in Fig. 9(b) and Fig. 9(c), and the values of LOS power ratio in Fig. 9(d) are small, because of the small Tx-Rx distance at the position 7-9, 10, 17 and 18.

Especially, the large deviation in the values of delay spread, angle spread, and LOS power ratio as shown in Fig. 9(b)-9(d) at position 8 and 14, are mostly due to the distance between Tx and Rx. According to PADPs of position 8 and 14 obtained by the HRPE algorithm shown in Fig. 10, the main specular components after the LOS path are sparse. Besides that, the strong reflections at position 8 are mainly from the white pillars and yellow ventilation tubes nearby as shown in Fig. 10(a) with small range of azimuth, while mainly from the walls around at Tx position 14 in Fig. 10(b) with large range of azimuth.

E. DISCUSSION

The channel characteristics summarized in Table 2 provide us with the similarities and difference between the propagation channels in different scenarios.

TABLE 2. Summary of the characteristic parameters.

Room	R1-Classroom	R2-Classroom	R3-Office	R4-Hall
Decay factor (ns)	26.33-49.51	23.73-24.66	8.90-11.15	N/A
Delay Spread (ns)	37.89-62.55	23.57-24.18	11.76-13.15	53.82-83.78
Angle Spread (°)	36.81-59.64	45.40-62.68	24.63-40.33	12.75-35.12
LOS power ratio (dB)	0.14-7.67	-2.95-(-1.81)	2.92-5.88	8.07-13.42

It can be found that the characteristic parameters are closely related to the room size of the scenarios. The values of the decay factor are similar in the same classroom of two scenarios, while the values in R3-Office are much lower, due to the small volume of the office. The diffuse spectrum can be observed in small room size of R3-Office, while in large dimension of R4-hall scenario, there is little diffuse spectrum observed, resulting in no decay factor.

The large values of the delay spread are observed in R4-Hall scenario, and smallest values of delay spread are seen in R3-Office with small room size. The values of delay spread in R1-Classroom are larger than that in R2-Classroom with the same room size, because of strong reflection from the poles of the blackboard in R2-Classroom. The LOS dominance and specular components are most apparent in open hall environment, according to the highest values of LOS power ratio.

The results of the measurements with Tx antenna at different positions in R1-Classroom and R4-Hall scenarios indicate that the characteristic parameters are also associated with the antenna locations in the scenario. The values of characteristic parameters are significantly affected by the antenna locations, due to the strong reflections from the objects, walls and corners around the antenna. As the Tx antenna was located in the corner of the R2-Classroom, there are strong reflection components from the poles of the blackboard in the corner, leading to the values of LOS power ratio in R2-Classroom lower than the values in other scenarios, presenting the NLOS dominance in R2-Classroom.

As ray tracing simulation mainly suffers from inaccurate database and computational complexity. The room furniture richness level on the characteristic parameters of the propagation channel is also investigated. This is beneficial for ray tracing simulation as detailed database description might not be needed in some scenarios. Our observation is that furniture richness might in some cases not relevant to the channel parameters. Since the channel parameters derived here may be dominated by the LOS path, the impact of furniture richness on channels may be interesting to consider the analysis in case of NLOS and obstructed-LOS as well in the further.

V. CONCLUSION

In this contribution, four indoor measurements in classrooms, office and hall were conducted at the frequency band of 27 GHz-29 GHz. Channel characteristics, i.e. decay factor, delay spread, angle spread and line of sight (LOS) power ratio, were investigated and compared in different scenarios.

The channel characteristics differ in different scenarios. It is found that the values of the delay spread in R4-Hall are much larger than that in R3-Office, and values of angle spread in R4-Hall are much smaller than that in R3-Office. It reveals that the size of the indoor scenarios has significant impact on the channel characteristics. In individual scenarios, the channel characteristics vary with respect to different Tx locations, which can be seen from the apparent fluctuation of the channel characteristics at different Tx position in R1-Classroom and R4-Hall. Furthermore, in R2-Classroom and R3-Office, little fluctuation of the channel characteristics can be found with the furniture removing step by step, which indicates weakly impact of the furniture richness in indoor scenario on channel propagation. Generally speaking, the LOS and specular propagation mechanisms are dominant at 27 GHz-29 GHz mm-wave band, especially more apparent in large R4-Hall scenario. In addition, it is interested to notice the value of LOS power ratio in R2-Classroom is much lower than that in R1-Classroom. That is caused by the strong reflection from the aluminous poles of the blackboard in the corner Tx located in R2-Classroom.

ACKNOWLEDGMENT

The authors would like to thank Yiming Zhang for modifying the paper.

REFERENCES

[1] T. S. Rappaport *et al.*, "Millimeter wave mobile communications for 5G cellular: It will work!" *IEEE Access*, vol. 1, pp. 335–349, May 2013.
[2] S. Salous *et al.*, "Millimeter-Wave Propagation: Characterization and modeling toward fifth-generation systems. [wireless corner]," *IEEE Antennas Propag. Mag.*, vol. 58, no. 6, pp. 115–127, Dec. 2016.
[3] Y. Niu, Y. Li, D. Jin, L. Su, and A. V. Vasilakos, "A survey of millimeter wave communications (mmWave) for 5G: Opportunities and challenges," *Wireless Netw.*, vol. 21, no. 8, pp. 2657–2676, Nov. 2015, 10.1007/s11276-015-0942-z.
[4] R. He, B. Ai, G. L. Stüber, G. Wang, and Z. Zhong, "Geometrical-based modeling for millimeter-wave MIMO mobile-to-mobile channels," *IEEE Trans. Veh. Technol.*, vol. 67, no. 4, pp. 2848–2863, Apr. 2018.
[5] T. S. Rappaport, Y. Xing, G. R. MacCartney, A. F. Molisch, E. Mellios, and J. Zhang, "Overview of millimeter wave communications for fifth-generation (5G) wireless networks—With a focus on propagation models," *IEEE Trans. Antennas Propag.*, vol. 65, no. 12, pp. 6213–6230, Dec. 2017.
[6] C. T. Neil, M. Shafi, P. J. Smith, P. A. Dmochowski, and J. Zhang, "Impact of microwave and mmwave channel models on 5G systems performance," *IEEE Trans. Antennas Propag.*, vol. 65, no. 12, pp. 6505–6520, Dec. 2017.
[7] J. Zhang, P. Tang, L. Tian, Z. Hu, T. Wang, and H. Wang, "6–100 GHz research progress and challenges from a channel perspective for fifth generation (5G) and future wireless communication," *Sci. China Inf. Sci.*, vol. 60, no. 8, pp. 080301-1–080301-18, 2017, doi: 10.1007/s11432-016-9144-x.

[8] K. Guan *et al.*, "Towards realistic high-speed train channels at 5G millimeter-wave band—Part I: Paradigm, significance analysis, and scenario reconstruction," *IEEE Trans. Veh. Technol.*, vol. 67, no. 10, pp. 9112–9128, Oct. 2018.

[9] D. He *et al.*, "Channel measurement, simulation, and analysis for high-speed railway communications in 5G millimeter-wave band," *IEEE Trans. Intell. Transp. Syst.*, vol. 19, no. 10, pp. 3144–3158, Oct. 2018.

[10] M. Kyrö, V. M. Kolmonen, and P. Vainikainen, "Experimental propagation channel characterization of mm-wave radio links in urban scenarios," *IEEE Antennas Wireless Propag. Lett.*, vol. 11, pp. 865–868, 2012.

[11] P. F. M. Smulders, "Statistical characterization of 60-GHz indoor radio channels," *IEEE Trans. Antennas Propag.*, vol. 57, no. 10, pp. 2820–2829, Oct. 2009.

[12] T. S. Rappaport, J. N. Murdock, and F. Gutierrez, Jr., "State of the art in 60-GHz integrated circuits and systems for wireless communications," *Proc. IEEE*, vol. 99, no. 8, pp. 1390–1436, Aug. 2011.

[13] C. Gustafson, K. Haneda, S. Wyne, and F. Tufvesson, "On mm-wave multipath clustering and channel modeling," *IEEE Trans. Antennas Propag.*, vol. 62, no. 3, pp. 1445–1455, Mar. 2014.

[14] T. S. Rappaport, G. R. Maccartney, M. K. Samimi, and S. Sun, "Wideband millimeter-wave propagation measurements and channel models for future wireless communication system design," *IEEE Trans. Commun.*, vol. 63, no. 9, pp. 3029–3056, Sep. 2015.

[15] K. Haneda, J. Järveläinen, A. Karttunen, M. Kyrö, and J. Putkonen, "A statistical spatio-temporal radio channel model for large indoor environments at 60 and 70 GHz," *IEEE Trans. Antennas Propag.*, vol. 63, no. 6, pp. 2694–2704, Jun. 2015.

[16] Y. Azar *et al.*, "28 ghz propagation measurements for outdoor cellular communications using steerable beam antennas in New York city," in *Proc. IEEE Int. Conf. Commun. (ICC)*, Jun. 2013, pp. 5143–5147.

[17] H. Zhao *et al.*, "28 GHz millimeter wave cellular communication measurements for reflection and penetration loss in and around buildings in New York city," in *Proc. IEEE Int. Conf. Commun. (ICC)*, Jun. 2013, pp. 5163–5167.

[18] M. K. Samimi *et al.*, "28 GHz angle of arrival and angle of departure analysis for outdoor cellular communications using steerable beam antennas in New York City," in *Proc. IEEE 77th Veh. Technol. Conf. (VTC Spring)*, Jun. 2013, pp. 1–6.

[19] J. Ko *et al.*, "Millimeter-wave channel measurements and analysis for statistical spatial channel model in in-building and urban environments at 28 GHz," *IEEE Trans. Wireless Commun.*, vol. 16, no. 9, pp. 5853–5868, Sep. 2017.

[20] P. Hanpinitsak, K. Saito, W. Fan, J.-I. Takada, and G. F. Pedersen, "Frequency characteristics of path loss and delay-angular profile of propagation channels in an indoor room environment in SHF bands," IEICE, Tokyo, Japan, Tech. Rep. SRW2016-96, Mar. 2017.

[21] W. Fan, I. Carton, J. Ø. Nielsen, K. Olesen, and G. F. Pedersen, "Measured wideband characteristics of indoor channels at centimetric and millimetric bands," *EURASIP J. Wireless Commun. Netw.*, vol. 2016, no. 1, p. 58, Feb. 2016, 10.1186/s13638-016-0548-x.

[22] Ainfoinc. (Jun. 5, 2018). *SZ-2003000-P.pdf*. [Online]. Available: http://www.ainfoinc.com/en/pro_pdf/new_products/antenna/Bi-Conical%20Antenna/tr_SZ-2003000-P.pdf

[23] S. S. Zhekov, A. Tatomirescu, and G. F. Pedersen, "Antenna for ultrawideband channel sounding," *IEEE Antennas Wireless Propag. Lett.*, vol. 16, pp. 692–695, 2017.

[24] G. Steinböck, T. Pedersen, B. H. Fleury, W. Wang, and R. Raulefs, "Experimental validation of the reverberation effect in room electromagnetics," *IEEE Trans. Antennas Propag.*, vol. 63, no. 5, pp. 2041–2053, May 2015.

[25] A. Bamba *et al.*, "Experimental assessment of specific absorption rate using room electromagnetics," *IEEE Trans. Electromagn. Compat.*, vol. 54, no. 4, pp. 747–757, Aug. 2012.

[26] X. Cai, X. Yin, X. Cheng, and A. P. Yuste, "An empirical random-cluster model for subway channels based on passive measurements in UMTS," *IEEE Trans. Commun.*, vol. 64, no. 8, pp. 3563–3575, Aug. 2016.

[27] X. Cai and W. Fan, "A complexity-effcient high resolution propagation parameter estimation algorithm for ultra-wideband large-scale uniform circular array," *IEEE Trans.*, to be published.

[28] 3GPP, *Study on Channel Model for Frequencies from 0.5 to 100 GHz*, document TR25.996 version 14.0.0 Release 14), 3GPP, 2018.

GUOJIN ZHANG received the bachelor's degree in information engineering from the China University of Mining and Technology, China, in 2013, and the master's degree from the China University of Petroleum (East China), China, in 2016. From 2016 to 2018, she was with Ericsson Communications, China, as a Network Engineer. She is currently a Guest Ph.D. Researcher with the Antennas, Propagation and Millimeterwave Systems Section, Aalborg University, Denmark. The focus of her work is on channel parameter estimation and radio propagation channel modeling in millimeter wave frequency bands.

KENTARO SAITO was born in Kanagawa, Japan, in 1977. He received the B.S. and Ph.D. degrees from The University of Tokyo, Japan, in 2002 and 2008, respectively. He joined NTT DOCOMO, Yokosuka, Kanagawa, in 2002. Since then, he has been engaged in the research and development of mobile communication systems, and radio propagation. He joined Tokyo Institute of Technology, Japan, in 2015. Since then, he has been engaged in research on radio propagation for mobile communication systems.

Dr. Saito is a member of the IEICE.

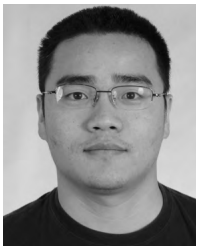

WEI FAN received the B.E. degree from the Harbin Institute of technology, China, in 2009, the master's double degree (Hons.) from the Politecnico di Torino, Italy, and the Grenoble Institute of Technology, France in 2011, and the Ph.D. degree from Aalborg University, Denmark, in 2014. In 2011, he was with Intel Mobile Communications, Denmark, as a Research Intern. He conducted a three-month internship at Anite telecoms oy, Finland, in 2014. He is currently an Associate Professor with the Antennas, Propagation and Millimeterwave Systems Section, Aalborg University. His main areas of research are over the air testing of multiple antenna systems, radio channel sounding, modeling, and emulation.

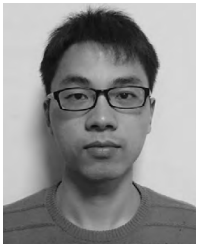

XUESONG CAI received the B.S. and Ph.D. degrees in electronics science and technology from Tongji University, Shanghai, China, in 2013 and 2018, respectively. He was also a Visiting Scholar with the Universidad Politecnica de Madrid, Madrid, Spain, in 2016. Since 2018, he has been a Post-Doctoral Fellow with the Antenna, Propagation and Millimetre-Wave Systems Section, Department of Electronic Systems, Faculty of Engineering and Science, Aalborg University, Aalborg, Denmark. His research interests are propagation channel measurement, parameter estimation, characterization, and modeling. He received the National Scholarship for Ph.D. Candidates, received the title of Excellent Student in 2016, the title of Excellent Student for the celebration of Tongji University's 110th anniversary, the ZTE Fantastic Algorithm Award in 2017, and the title of Outstanding Doctorate Graduate from the Shanghai Municipal Education Commission in 2018.

PANAWIT HANPINITSAK (S'17) was born in 1991. He received the B.E. degree (Hons.) in electronics and communications engineering from the Sirindhorn International Institute of Technology, Thammasat University, Pathumthani, Thailand, in 2013, and the M.E. degree in international development engineering major in electrical/electronics engineering from the Tokyo Institute of Technology, Japan, in 2016, where he is currently pursuing the D.E. degree. He was a Guest Ph.D. Researcher with Aalborg University, Denmark, and the Ilmenau University of Technology, Germany, in 2016 and 2018, respectively. His research interests include channel parameter estimation and beamforming algorithms, and radio propagation channel modeling at millimeter waves. He received the Best Student Presentation Award from the IEICE Short Range Wireless conference in 2017. He is a Student Member of the IEICE.

JUN-ICHI TAKADA (S'89–M'93–SM'11) received the B.E., M.E., and D.E. degrees in electrical and electronic engineering from the Tokyo Institute of Technology, Tokyo, Japan, in 1987, 1989, and 1992, respectively. From 1992 to 1994, he was a Research Associate with Chiba University, Chiba, Japan. From 1994 to 2006, he was an Associate Professor with the Tokyo Institute of Technology, where he has been a Professor since 2006. From 2003 to 2007, he was also a Researcher with the National Institute of Information and Communications Technology, Kyoto, Japan. From 2007 to 2010, he was a Co-Chair of the Special Interest Group on Body Communications within EU COST Action 2100. His research interests include radio-wave propagation and channel modeling for mobile and short range wireless systems, regulatory issues of spectrum sharing, and ICT applications for international development. He was an appointed IEICE Fellow in 2012. He was a recipient of the Achievement Award at IEICE in 2008.

GERT FRØLUND PEDERSEN was born in 1965 and married to Henriette and have seven children. He received the B.Sc.E.E. degree (Hons.) in electrical engineering from the College of Technology, Dublin, Ireland, in 1991, and the M.Sc.E.E. and Ph.D. degrees from Aalborg University in 1993 and 2003, respectively. Since 1993, he has been with Aalborg University, where he is currently a Full Professor heading the Antenna, Propagation and Networking LAB with 36 researcher. He is also the Head of the doctoral school on wireless communication with some 100 Ph.D. students enrolled. He has published more than 175 peer-reviewed papers and holds 28 patents. He has also worked as consultant for developments of more than 100 antennas for mobile terminals, including the first internal antenna for mobile phones in 1994 with lowest SAR, first internal triple-band antenna in 1998 with low SAR, and high TRP and TIS, and lately various multi antenna systems rated as the most efficient on the market. He has worked most of the time with joint university and industry projects and have received more than 12 M$ in direct research funding. He is the Project Leader of the SAFE project with a total budget of 8 M$ investigating tunable front end, including tunable antennas for the future multiband mobile phones. He has been one of the pioneers in establishing over-the-air (OTA) measurement systems. The measurement technique is now well established for mobile terminals with single antennas and he was chairing the various COST groups (swg2.2 of COST 259, 273, 2100 and now ICT1004) with liaison to 3GPP for OTS test of MIMO terminals. He is deeply involved in MIMO OTA measurement. His research has focused on radio communication for mobile terminals especially small antennas, diversity systems, propagation and biological effects.